Nonlinear Modal Substructuring of Panel and Stiffener Assemblies via Characteristic Constraint Modes

Joseph D. Schoneman,[1] Matthew S. Allen,[2] and Robert J. Kuether[3]

[1]Engineer, ATA Engineering; email: joe.schoneman@ata-e.com

[2]Assistant Professor, University of Wisconsin – Madison; email: matt.allen@wisc.edu

[3]Senior Member of Technical Staff, Sandia National Laboratories*; email: rjkueth@sandia.gov

Abstract

Thin beams and panels subjected to large loadings will behave nonlinearly due to membrane stretch effects as they approach deflections on the order of their thickness; this behavior can be efficiently and accurately modeled using nonlinear reduced order models based on the structure's linear normal modes. However, the complexity of such reduced order models grows cubically with the number of linear modes in the basis set, making complicated geometries prohibitively expensive to compute. Component mode synthesis techniques may be used to reduce this cost by assembling a set of smaller nonlinear subcomponent models, each of which can be more quickly computed than a nonlinear model of the entire structure. Since geometric nonlinearity is heavily dependent on each structure's boundary conditions, however, subcomponents of an assembly which are constrained only at their interfaces – such as panels mounted to an underlying frame – prove difficult to treat using existing nonlinear modeling techniques. This work uses Craig-Bampton dynamic substructuring combined with characteristic constraint modes for interface reduction to examine the challenges associated with panel and frame assemblies, with a simple example motivating a discussion of current solutions and future challenges.

Keywords: Nonlinear Reduced Order Models, Dynamic Substructuring, Characteristic Constraint Modes

1 MOTIVATION

Linear analysis techniques form the foundation of modern structural dynamics. Most structures behave linearly at low levels of dynamic excitation, but certain high performance applications require low mass designs to withstand high environmental loads, causing responses in the nonlinear regime. It has long been possible to compute the response of geometrically nonlinear structures in finite element (FE) software, but the computational cost is orders of magnitude higher than that for linear analysis of the same structure. State-of-the-art FE software combined with high performance computing clusters allow multi-physics simulations with extremely complicated models - millions of degrees of freedom - to be performed in a reasonable amount of time: several hours to several days, depending on the model complexity and physics involved. This capability is extremely powerful, but such analysis times still limit the amount of design insight which can be obtained from a model. For applications requiring hundreds or thousands of analyses, such as optimization studies or Monte Carlo uncertainty quantification, day-long simulation times are not acceptable.

*Sandia National Laboratories is a multi-mission laboratory managed and operated by Sandia Corporation, a wholly owned subsidiary of Lockheed Martin Corporations, for the U.S. Department of Energy's National Nuclear Security Administration under Contract DE-AC04-94AL85000.

Specific motivating cases include skin panels of hypersonic vehicles[1], which undergo severe thermoacoustic loadings at cruising speeds in excess of Mach 5, as well as the ducted engine assemblies of stealth aircraft, where jet exhaust impinges directly on the structure. More recently, the spaceflight companies Blue Origin and Space Exploration Technologies Corporation have demonstrated the recovery of suborbital and first-stage orbital boosters, respectively. As each company moves forward with plans to land even larger stages, high-amplitude response of thin-walled booster structures may be a subject of increasing interest. Geometric nonlinearity is also significant in the analysis of joined-wing concepts[2] and in the behavior of extremely lightweight space structures such as solar sails[3]. Another application of interest is the "digital twin" concept under examination by the United States Air Force, which proposes the simulation of an entire aircraft over its flight history in near-realtime[4]. Full-order coupled simulation of the thermal, aerodynamic, and nonlinear structural physics of an aircraft is still barely (if at all) feasible, let alone achievable in real-time.

1.1 Nonlinear Reduced Order Models

For these and other scenarios in which rapid analysis of a structure is required, reduced order models (ROMs) are a common solution. A subset of basis vectors is used to model the structure's dynamics in a reduced space. When the full order structural model is treated as linear, the system's eigenvectors have unique properties that allow the equations of motion to be decoupled and solved analytically in either the time or frequency domain. This results in a reduction of the model by truncating the number of modes used to superpose the response. In the nonlinear case, numerical integration is the only generally applicable method to obtain a solution for a structure's equations of motion. In this scenario, reducing the order of a model is of even greater interest, as it dramatically reduces the cost of integration. The complication lies in accurately representing the nonlinear behavior of the full-order model in the reduced space, a task which is not straightforward to accomplish in comparison to linear structures. Proper model reduction of nonlinear systems is domain-dependent and closely linked to the type of nonlinearity being modeled. In this work, large-deflection nonlinearities of thin structures are considered; the nonlinearity of interest arises when the bending of a beam or plate couples into membrane stretching along the axis of the structure.

The earliest known presentation of large-deflection nonlinear reduced order modeling (NLROM) techniques is that by Nash[5] in 1977, with other early work in the field put forward by Segalman and Dorhmann[6][7], McEwan[8], and Muravyov and Rizzi[9]. A review of work in the field was performed by Mignolet et al.[10] in 2013. Nonlinearities are usually represented as a series of quadratic and cubic terms in the modal coordinates, which are often obtained by leveraging the nonlinear analysis capabilities of commercial finite element software. A low-order subset of linear modes is selected for inclusion in the NLROM basis; a series of nonlinear static finite element analyses then characterizes the nonlinear effects of membrane stretching. Forces (deflections) are applied in the shapes of a selected modal basis, and the resulting deflections (forces) from the finite element analysis are used to determine suitable coefficients for nonlinear terms in the NLROM. The technique used for this study is given by Gordon and Hollkamp[1][11]. In those works, nonlinear model reduction of a single structure was performed, but in this paper, the model reduction techniques are performed on individual components which are later assembled. Models generated using the former, more conventional approach are referred to here as "monolithic NLROMs" and will be used to validate the substructured NLROMs created in Section 4.3.

1.2 Component Mode Synthesis

For complicated structural assemblies, submodels of each component are often created independently and later assembled to form a model of the full assembly. The Craig-Bampton (CB) technique[12], with fixed-interface (FI) modes to model internal deformations and constraint modes to model boundary deformations, is an extremely common method for so-called component mode synthesis (CMS), although many other techniques exist. In the linear case, substructuring approaches are often used to enable the reuse of repeated components in an assembly, to couple numerical finite element models (FEMs) with experimentally-obtained representations of complex components, or to pass structural models between organizations without exposing proprietary design information. While such motivations are important, the key objective in this work is to use nonlinear CMS in order to obtain NLROMs that would be infeasible to construct directly from the assembled model. The computational cost of constructing an NLROM grows cubically with the number of basis vectors retained. Models containing several tens of modes become unwieldy to construct, and models containing as few as a hundred modes require so many static load cases that the NLROM is not competitive with full-order time integration, particularly when validation time and the process of selecting NLROM basis vectors is factored in.

If an assembly can be represented using a collection of lower-order NLROMs, then the computation requirements become quite reasonable. Kuether[13][14][15] demonstrated the application of nonlinear CMS techniques using several examples, most notably

a pair of plates pinned about their edges and joined at a common edge, as shown in Figure 1(a). This assembly is a simplification of a more realistic model for an aircraft skin, where thin skin panels are supported by an underlying frame composed of stringers and longerons. In many applications, fixed or pinned boundary conditions may not be sufficiently accurate to model these structures adequately. Unfortunately, several challenges arise when attempting to construct a component NLROM of a skin panel that is supported by stiffeners: not only does the free-free nature of the panel in its unassembled state cause challenges for obtaining static FE solutions, but the nonlinearity in each component is largely dependent on the stiffness of its supporting structure. To accurately model component nonlinearities, this boundary stiffness must be adequately accounted for.

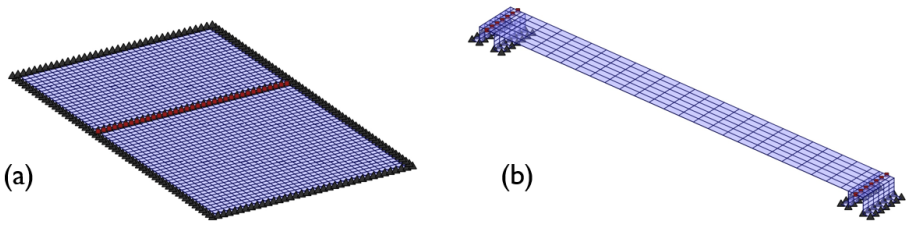

Figure 1: *(a) Two-panel model examined by Kuether[15]; note that each panel is fully constrained in its unassembled state. (b) Assembled beam/stiffener model studied here; the beam component is free-free when unassembled. In both images, black triangles denote boundary conditions while red squares denote coupling points.*

This paper extends Kuether's work by examining a truncated panel section mounted on two stiffeners, shown in Figure 1(b) – perhaps the simplest example which will demonstrate the relevant difficulties. The underlying theory for linear and nonlinear component mode synthesis is outlined in Sections 2 and 3 before moving on to the case study in Section 4.

2 LINEAR COMPONENT MODE SYNTHESIS

The theoretical development of Craig-Bampton component mode synthesis[12] is quite mature and not presented here. The characteristic constraint (CC) mode concept is a more recent development[16], but is also omitted for brevity; only a description of each component's reduced model is provided. The system of interest consists of n components and a total of N degrees of freedom (DOF). The j^{th} component is represented in full-order form by the undamped equation of motion (1)

$$\mathbf{M}^j\ddot{\mathbf{x}}^j + \mathbf{K}^j\mathbf{x}^j = \mathbf{f}^j \tag{1}$$

with mass matrix $\mathbf{M}^j$, stiffness matrix $\mathbf{K}^j$, forcing vector $\mathbf{f}^j$, and physical displacement vector $\mathbf{x}^j$ with N^j degrees of freedom. The double-overdot operator refers to the second derivative of each element with respect to time. Damping is omitted from this formulation; however, linear damping terms may easily be included. A variety of methods exist to calculate damping, but the most common rely on estimation or measurement of a damping ratio ζ for each mode. In the substructuring context, the damping ratios of each component may be estimated individually and assembled to obtain a system damping matrix, or the damping may be added using modes of the full assembly. Since the validation metric used here (described in Section 3.6) operates on the conservative model of the structure, no further consideration is given to damping.

The Craig-Bampton CMS technique reduces the order of Equation (1) while placing it in a form amenable to substructuring with other components in the system. The system-level use of CC modes further reduces the order of the model by performing a secondary modal reduction on the assembled boundary degrees of freedom of the structure. First, the j^{th} component's displacements are represented in Craig-Bampton form by

$$\begin{Bmatrix}\mathbf{x}_i^j\\ \mathbf{x}_b^j\end{Bmatrix} = \begin{bmatrix}\mathbf{\Psi}_{ik}^j & \mathbf{\Psi}_{ib}^j\\ \mathbf{0}_{bk}^j & \mathbf{I}_{bb}^j\end{bmatrix}\begin{Bmatrix}\mathbf{q}_k^j\\ \mathbf{x}_b^j\end{Bmatrix} = \mathbf{T}_{CB}^j\begin{Bmatrix}\mathbf{q}_k^j\\ \mathbf{x}_b^j\end{Bmatrix} \tag{2}$$

where the internal degrees of freedom $\mathbf{x}_i^j$ are modeled with a combination of k fixed interface modes $\mathbf{\Psi}_{ik}^j$ and constraint modes

$\mathbf{\Psi}_{ib}^j$ with corresponding modal amplitudes $\mathbf{q}_k^j$ and boundary degrees of freedom $\mathbf{x}_b^j$. Once each component model is available, the structure is assembled; however, a large number of boundary DOF will still be present if the components feature large component boundaries. The characteristic constraint modal reduction is used to alleviate this issue. At the assembly level, the Craig-Bampton degrees of freedom are expressed as

$$\begin{Bmatrix} \mathbf{q}_{\hat{k}} \\ \mathbf{q}_{\hat{b}} \end{Bmatrix} = \begin{bmatrix} \mathbf{I}_{\hat{k}\hat{k}} & \mathbf{0}_{\hat{k}C} \\ \mathbf{0}_{C\hat{k}} & \hat{\mathbf{\Psi}}_{CC} \end{bmatrix} \begin{Bmatrix} \mathbf{q}_{\hat{k}} \\ \mathbf{q}_{CC} \end{Bmatrix} \tag{3}$$

where $\mathbf{q}_{\hat{k}}$ is the collection of FI modal amplitudes, $\mathbf{q}_{\hat{b}}$ is the set of boundary DOF, $\hat{\mathbf{\Psi}}_{CC}$ is the CC modal matrix and $\mathbf{q}_{CC}$ is the CC amplitude vector. To make use of this transformation using nonlinear reduced order models, the global CC modes must be "localized" to each component; the boundary DOF of the j^{th} component are denoted in terms of the CC modal matrix by $\mathbf{x}_b^j = \{\hat{\mathbf{\Psi}}_{CC}\}^j \mathbf{q}_{CC}$. This leads to a component-level model in terms of the FI and CC modes,

$$\begin{Bmatrix} \mathbf{x}_i^j \\ \mathbf{x}_b^j \end{Bmatrix} = \begin{bmatrix} \mathbf{\Psi}_{ik}^j & \mathbf{\Psi}_{ib}^j \{\hat{\mathbf{\Psi}}_{CC}\}^j \\ \mathbf{0}_{bk}^j & \{\hat{\mathbf{\Psi}}_{CC}\}^j \end{bmatrix} \begin{Bmatrix} \mathbf{q}_k^j \\ \mathbf{q}_{CC} \end{Bmatrix} \tag{4}$$

This transformation matrix can be used as a basis for generating nonlinear reduced order models, as described below.

3 EXTENSION TO GEOMETRICALLY NONLINEAR STRUCTURES

The substructuring approach is now extended to admit geometrically nonlinear restoring forces. An explanation of the implicit condensation and expansion (ICE) method[1][11] as implemented in this work is presented. The assembly procedure itself follows, along with a discussion on the use of alternative basis vectors to represent the nonlinear restoring force vector.

3.1 Component-Level Nonlinearity

Consider the application of the aforementioned substructuring techniques to structures involving nonlinear forces. Each conservative component equation of motion is now

$$\mathbf{M}^j \ddot{\mathbf{x}}^j + \mathbf{K}^j \mathbf{x}^j + \mathbf{f}_{nl}^j(\mathbf{x}^j) = \mathbf{f}^j \tag{5}$$

with $\mathbf{f}_{nl}^j(\mathbf{x}^j)$ a nonlinear restoring force vector associated with the geometric nonlinearity of the system. Given a modal reduction matrix and corresponding set of generalized coordinates $\mathbf{x}^j = \mathbf{\Phi}^j \mathbf{q}^j$, where $\mathbf{\Phi}^j$ is a matrix of FI and component-localized CC modes and $\mathbf{q}^j$ are their modal coordinates, the reduced system becomes

$$\bar{\mathbf{M}}^j \ddot{\mathbf{q}}^j + \bar{\mathbf{K}}^j \mathbf{q}^j + \boldsymbol{\theta}^j(\mathbf{q}^j) = \bar{\mathbf{f}}^j \tag{6}$$

The transformed load vector is $\bar{\mathbf{f}}^j = (\mathbf{\Phi}^j)^T \mathbf{f}^j$ and the reduced system matrices are $\bar{\mathbf{M}}^j = (\mathbf{\Phi}^j)^T \mathbf{M}^j (\mathbf{\Phi}^j)$ and $\bar{\mathbf{K}}^j = (\mathbf{\Phi}^j)^T \mathbf{K}^j (\mathbf{\Phi}^j)$. For Craig-Bampton models using characteristic constraint modes, $\mathbf{\Phi}^j$ will contain the component's fixed-interface modes along with the local partition of the system's characteristic constraint modes; in this case the reduced mass matrix will not be diagonal. The component stiffness matrix is not necessarily diagonalized by the local partition of system CC modes, but the block corresponding to the FI modes will at least be diagonal.

The nonlinear force, when transformed to the modal domain, becomes $\boldsymbol{\theta}^j(\mathbf{q}^j) = (\mathbf{\Phi}^j)^T \mathbf{f}_{nl}^j(\mathbf{\Phi}^j \mathbf{q}^j)$. The physical-coordinate form of this force, $\mathbf{f}_{nl}^j$, is never actually considered. Instead, the r^{th} term in the nonlinear modal restoring force vector is known to take the form

$$\boldsymbol{\theta}_r^j(q_1^j, q_2^j, ..., q_m^j) = \sum_{i=1}^{m}\sum_{k=1}^{m} B_r^j(i,k) q_i^j q_k^j + \sum_{i=1}^{m}\sum_{k=1}^{m}\sum_{l=1}^{m} A_r^j(i,j,k) q_i^j q_k^j q_l^j \tag{7}$$

The summation index m indicates the number of basis vectors in $\boldsymbol{\Phi}^j$. The arrays A_r^j and B_r^j contain quadratic and cubic stiffness coefficients of the nonlinear model; specification of these coefficients provides complete determination of the NLROM. Two key approaches exist to perform this task; the ICE method[17] is used here, although the enforced displacement technique[9] is also popular. Using ICE, a series of static loads are applied to the full order model, each one a linear combination of the basis vectors in $\boldsymbol{\Phi}^j$. These are pre-multiplied by the stiffness matrix to better isolate individual modes. Hence, the vectors $\mathbf{f}_A$, used to identify cubic stiffness coefficients, and $\mathbf{f}_B$, used to identify quadratic stiffness coefficients, are defined in terms of basis vectors of index r, s, and v as

$$\begin{aligned} \mathbf{f}_A &= \frac{1}{3}\mathbf{K}^j \left[f_r\{\boldsymbol{\Phi}^j\}_r + f_s\{\boldsymbol{\Phi}^j\}_s + f_v\{\boldsymbol{\Phi}^j\}_v \right] \\ \mathbf{f}_B &= \frac{1}{2}\mathbf{K}^j \left[f_r\{\boldsymbol{\Phi}^j\}_r + f_s\{\boldsymbol{\Phi}^j\}_s \right] \end{aligned} \tag{8}$$

with a separate load scaling term f_r, f_s, and f_v for each mode in the basis. The indices r, s, and v need not be unique, and the fractional factors are included so that loadings including, for example, three instances of the r^{th} mode, will have an effective scaling factor of f_r rather than $3f_r$. Selection of these load scaling terms is critical for an accurate fit of the nonlinear coefficients, since weak loadings will not sufficiently exercise the structural nonlinearities, but strong loadings will lead to convergence issues in the FEA solution. Kuether et al.[18] showed that an effective rule for selecting force amplitudes is to scale them such that the nonlinear static FE solution deflects 15 to 20 percent less (more) than a purely linear static solution due to the hardening (softening) characteristic of the nonlinearity. Loads pushing the linear model of the structure to a one thickness displacement often satisfy this criterion. Thus, the load scaling factors can be defined using the thickness h, a deflection scaling factor α_r, and the set of single-mode loadings. For the r^{th} mode,

$$\begin{aligned} \mathbf{K}^j\mathbf{x}^j &= f_r\mathbf{K}^j\{\boldsymbol{\Phi}^j\}_r \\ \alpha_r h = \max|\mathbf{x}^j| &= \max|f_r\{\boldsymbol{\Phi}^j\}_r| \\ f_r &= \frac{\alpha_r h}{\max|\{\boldsymbol{\Phi}^j\}_r|} \end{aligned}$$

The resulting nonlinear deflection for each single-mode load case with the load scaling factor f_r can be compared to the value $\alpha_r h$, and α_r adjusted as needed until the linear/nonlinear ratio approaches 0.8 or 1.2.

Once the scaling factors are determined, a full set of load cases is generated and supplied to a nonlinear FEA code. The required number of load cases to specify all of the A_r^j and B_r^j coefficients has a cubic order of growth; the exact count can be determined from

$$2m + \frac{2m!}{(m-2)!} + \frac{4m!}{3(m-3)!} = \frac{2}{3}(2m^3 - 3m^2 + 4m) \tag{9}$$

3.2 Nash's Form of Nonlinear Restoring Force

The polynomial expression (7) is an explicit description of the nonlinear restoring force on a mode-by-mode basis, but a more compact representation is available due to Nash[5]. By defining the quadratic and cubic nonlinear force vectors as

$$\begin{aligned} \boldsymbol{\beta}^j(\mathbf{q}^j) \Rightarrow \beta_r^j(\mathbf{q}^j) &= \sum_{i=1}^{m}\sum_{k=1}^{m} B_r^j(i,k) q_i^j q_k^j \\ \boldsymbol{\alpha}^j(\mathbf{q}^j) \Rightarrow \alpha_r^j(\mathbf{q}^j) &= \sum_{i=1}^{m}\sum_{k=1}^{m}\sum_{l=1}^{m} A_r^j(i,j,k) q_i^j q_k^j q_l^j \end{aligned}$$

and taking the Jacobian of each so that $\mathbf{N}_1^j(\mathbf{q}^j) = \nabla\boldsymbol{\beta}^j(\mathbf{q}^j)$ and $\mathbf{N}_2^j(\mathbf{q}^j) = \nabla\boldsymbol{\alpha}^j(\mathbf{q}^j)$, the component equation of motion can be written

$$\bar{\mathbf{M}}^j\ddot{\mathbf{q}}^j + \left[\bar{\mathbf{K}}^j + \frac{1}{2}\mathbf{N}_1^j(\mathbf{q}^j) + \frac{1}{3}\mathbf{N}_2^j(\mathbf{q}^j)\right]\mathbf{q}^j = \mathbf{0}$$

which is a form amenable to assembly within a substructure of multiple components.

3.3 Assembly of Craig-Bampton/Characteristic Constraint Substructures

To proceed with actual assembly of the nonlinear forces, we must apply a procedure which differs somewhat from the linear assembly process. The full assembly equations of motion are

$$\hat{\mathbf{M}}_{CC}\ddot{\hat{\mathbf{q}}}_{CC} + \left[\hat{\mathbf{K}}_{CC} + \frac{1}{2}\hat{\mathbf{N}}_1(\hat{\mathbf{q}}_{CC}) + \frac{1}{3}\hat{\mathbf{N}}_2(\hat{\mathbf{q}}_{CC})\right]\hat{\mathbf{q}}_{CC} = \hat{\mathbf{f}}_{CC} \tag{10}$$

in which $\hat{\mathbf{N}}_1(\hat{\mathbf{q}}_{CC})$ are $\hat{\mathbf{N}}_2(\hat{\mathbf{q}}_{CC})$ the assembled nonlinear Jacobian matrices which we seek. Recall that the system degrees of freedom are written in terms of the component FI modal amplitudes $\mathbf{q}_k^j$ and the global CC modal amplitudes $\mathbf{q}_{CC}$,

$$\hat{\mathbf{q}}_{CC} = \begin{Bmatrix} \mathbf{q}_k^1 \\ \mathbf{q}_k^2 \\ \vdots \\ \mathbf{q}_k^n \\ \mathbf{q}_{CC} \end{Bmatrix}$$

Each characteristic constraint mode will enter the displacements of all components in the assembly. An "unassembled" vector of FI/CC coordinates can also be written:

$$\hat{\mathbf{q}}_{CC,u} = \begin{Bmatrix} \mathbf{q}_k^1 \\ \mathbf{q}_{CC} \\ \mathbf{q}_k^2 \\ \mathbf{q}_{CC} \\ \vdots \\ \mathbf{q}_k^n \\ \mathbf{q}_{CC} \end{Bmatrix} = \begin{Bmatrix} \mathbf{q}^1 \\ \mathbf{q}^2 \\ \vdots \\ \mathbf{q}^n \end{Bmatrix}$$

The assembled and unassembled coordinate vectors are related by $\hat{\mathbf{q}}_{CC} = \mathbf{L}_{CC}\hat{\mathbf{q}}_{CC,u}$. $\mathbf{L}_{CC}$ is an assembly matrix operating in the FI/CC domain, and can be constructed easily since all fixed interface modes are independent of each other and all characteristic constraint modes are constrained. This assembly matrix provides a framework for assembling the nonlinear restoring forces of each component. Similar to assembly of the linear system matrices, unassembled Jacobian matrices are block diagonal in terms of the component Jacobians,

$$\hat{\mathbf{N}}_{1,u}(\hat{\mathbf{q}}_{CC,u}) = \begin{bmatrix} \mathbf{N}_1^1(\mathbf{q}^1) & & & \\ & \mathbf{N}_1^2(\mathbf{q}^2) & & \\ & & \ddots & \\ & & & \mathbf{N}_1^n(\mathbf{q}^n) \end{bmatrix} \quad \hat{\mathbf{N}}_{2,u}(\hat{\mathbf{q}}_{CC,u}) = \begin{bmatrix} \mathbf{N}_2^1(\mathbf{q}^1) & & & \\ & \mathbf{N}_2^2(\mathbf{q}^2) & & \\ & & \ddots & \\ & & & \mathbf{N}_2^n(\mathbf{q}^n) \end{bmatrix} \tag{11}$$

The assembled Jacobian matrices are written

$$\begin{aligned} \hat{\mathbf{N}}_1(\hat{\mathbf{q}}_{CC}) &= \mathbf{L}_{CC}^T \hat{\mathbf{N}}_{1,u}(\mathbf{L}_{CC}\hat{\mathbf{q}}_{CC,u})\mathbf{L}_{CC} \\ \hat{\mathbf{N}}_2(\hat{\mathbf{q}}_{CC}) &= \mathbf{L}_{CC}^T \hat{\mathbf{N}}_{2,u}(\mathbf{L}_{CC}\hat{\mathbf{q}}_{CC,u})\mathbf{L}_{CC} \end{aligned} \tag{12}$$

3.4 Basis Vectors of the Nonlinear Restoring Force

Finally, the component transformation matrix $\mathbf{\Phi}^j$ corresponding to the FI/CC mode coordinates $\mathbf{q}^j$ must be specified. A natural choice for the basis transformation is the set of FI and CC vectors, as shown in Equation (4), so that

$$\mathbf{\Phi}^j = \begin{bmatrix} \mathbf{\Psi}_{ik}^j & \mathbf{\Psi}_{ib}^j \{\hat{\mathbf{\Psi}}_{CC}\}^j \\ \mathbf{0}_{bk}^j & \{\hat{\mathbf{\Psi}}_{CC}\}^j \end{bmatrix} \tag{13}$$

With this selection made, the overall process for computing and assembling an NLROM is summarized as follows:

- After the FI/CC substructuring procedure, partition the characteristic mode matrix and supply $\mathbf{\Phi}^j$ to each component.
- Set the load scaling factors f_r so that each single-mode load case, having the shape $\mathbf{K}^j\{\mathbf{\Phi}^j\}_r$, yields a nonlinear static deflection which differs from a linear static prediction by 15 to 20 percent. Linear displacements of one thickness provide a good starting point.
- Compute all possible permutations of the load cases from Equation (8), supply as static loads to a nonlinear FEA program, and curve-fit coefficients of the NLROM according to Equation (7). Each NLROM is now available at the component level.
- The nonlinear restoring force is assembled at each timestep for simulation. Each component NLROM is supplied with the FI and CC displacements $\mathbf{q}^j$ to compute the component Jacobian matrices; these are then assembled using Equation (12) and supplied to the equations of motion (10) to advance the system state.

Note from the last point that a nonlinear model of the full system is never explicitly created. A full assembly procedure could be accomplished with the aid of symbolic algebra software; however, such an approach is not taken in this work.

3.5 Nonlinear Force Definition with Alternative Basis Vectors

A critical aspect of the ICE algorithm is the process used to estimate modal displacements resulting from the nonlinear deflections obtained from FEA software. Suppose the matrix of displacements, obtained from an FE code, is denoted by $\mathbf{Y}$. When the usual approach is used[17] so that the load basis $\mathbf{\Phi}^j$ is orthogonal through the stiffness matrix, so that $(\mathbf{\Phi}^j)^T\mathbf{K}^j\mathbf{\Phi}^j = \mathbf{\Lambda}$ where $\mathbf{\Lambda}$ is a diagonal matrix with nonzero determinant, a left pseudo-inverse of $\mathbf{\Phi}^j$ can be written so that $[\mathbf{\Lambda}^{-1}(\mathbf{\Phi}^j)^T\mathbf{K}^j]\mathbf{\Phi}^j = \mathbf{I}$ and the modal displacements associated with the loading are $\mathbf{q}^j = [\mathbf{\Lambda}^{-1}(\mathbf{\Phi}^j)^T\mathbf{K}^j]\mathbf{Y}$.[1]

Unfortunately, orthogonality cannot be guaranteed for the basis vectors used here, which involve partitions of the system CC modes to individual components. As such, MATLAB's *pinv* routine was used generate a Moore-Penrose pseudo-inverse of $\mathbf{\Phi}^j$

[1] If the $\mathbf{\Phi}^j$ is orthogonal through the mass matrix $\mathbf{M}^j$, then $\mathbf{q}^j = (\mathbf{\Phi}^j)^T\mathbf{M}^j\mathbf{Y}$. This is not the case when a Craig-Bampton transformation is used.

to estimate modal amplitudes from the nonlinear FE results. It may be the case that $\mathbf{\Phi}^j$ is poorly conditioned – the localized CC modes may very closely resemble FI modes of that component, for instance – which causes difficulty in finding an accurate solution for the modal amplitudes. When the modal coefficients for a given set of forces cannot be accurately estimated, the least squares routine used to construct Equation (7) does not provide accurate estimates of the nonlinear restoring force coefficients, and the resulting NLROM is inaccurate or even unstable.

To circumvent this issue, alternate sets of basis vectors can be used in the static curve fit procedure. These sets should still span the subspace described by the FI and localized CC modes, but display orthogonality with respect to each other for better conditioning and more accurate estimation of the modal response amplitudes. Two decomposition strategies are immediately obvious: the singular value decomposition (SVD) and the QR decomposition. The former method seems attractive due to its natural sorting of basis vectors by singular value. However, it turns out that the singular values tend to be inversely proportional to the natural frequency, so that the SVD prioritizes the relatively unimportant high-frequency deformations over the low-frequency modes that are of interest in creating NLROMs. As such, only the QR decomposition is used to obtain an orthogonal basis of the FI/CC subspace. With this method, the initial matrix $\mathbf{\Phi}^j$ can be written

$$\mathbf{\Phi}^j = \mathbf{Q}^j\mathbf{R}^j = \begin{bmatrix}\mathbf{Q}_1^j & \mathbf{Q}_2^j\end{bmatrix}\begin{bmatrix}\mathbf{R}_1^j \\ \mathbf{0}\end{bmatrix} \tag{14}$$

so that

$$\mathbf{x}^j = \mathbf{\Phi}^j\mathbf{q}^j = \mathbf{Q}_1^j\mathbf{R}_1^j\mathbf{q}^j$$

where $\mathbf{Q}_1^j$ is orthogonal and $\mathbf{R}_1^j$ is upper triangular. Writing the amplitudes as $\boldsymbol{\eta}^j = \mathbf{R}_1^j\mathbf{q}^j$, the transformed basis vectors are contained in $\mathbf{Q}_1^j$:

$$\mathbf{x}^j = \mathbf{Q}_1^j\boldsymbol{\eta}^j$$

Static loads can be applied in the shape of the basis vectors of $\mathbf{Q}_1^j$ and used to evaluate the nonlinear restoring force coefficients in terms of those shapes. No matter whether the nonlinear force is represented using FI/CC coordinates or via the QR decomposition, the full assembly is still integrated using the FI/CC coordinates. At each timestep, each component's nonlinear restoring force is computed by

- Transforming from FI/CC coordinates to decomposition coordinates using $\boldsymbol{\eta}^j = \mathbf{\Gamma}^j\mathbf{q}^j$ (with $\mathbf{\Gamma}^j$ corresponding to either $\mathbf{\Gamma}_{SVD}^j$ or $\mathbf{\Gamma}_{QR}^j$).
- Using the identified coefficients to compute Jacobian matrices in the decomposed space; $\tilde{\mathbf{N}}_1^j(\boldsymbol{\eta}^j)$ and $\tilde{\mathbf{N}}_2^j(\boldsymbol{\eta}^j)$, with overtilde denoting that these matrices do not operate on FI/CC coordinates.
- Transforming the component Jacobian matrices back to FI/CC space as shown in Equation (15)

$$\begin{aligned}\mathbf{N}_1^j(\mathbf{q}^j) &= (\mathbf{\Gamma}^j)^T\tilde{\mathbf{N}}_1^j(\boldsymbol{\eta}^j)\mathbf{\Gamma}^j \\ \mathbf{N}_2^j(\mathbf{q}^j) &= (\mathbf{\Gamma}^j)^T\tilde{\mathbf{N}}_2^j(\boldsymbol{\eta}^j)\mathbf{\Gamma}^j\end{aligned} \tag{15}$$

The linear model of each component remains in the untransformed FI/CC space. Once each component's nonlinear restoring force is evaluated, assembly proceeds as usual via Equation (12).

3.6 Nonlinear Normal Modes for Model Validation

To validate the NLROMs constructed in Section 4, the nonlinear normal mode (NNM) concept is applied to check for dynamic equivalence of the full-order and reduced models. Two main definitions of the NNM exist. The first, due to Rosenberg[19], defines an NNM as a *vibration in unison* of a system. This can be interpreted as a straightforward generalization of linear normal modes to nonlinear systems; however, it is not rigorously applicable to damped structures. To discuss NNMs in the context of nonconservative systems, Shaw and Pierre define a nonlinear normal mode as an invariant manifold in phase space[20]. Periodic orbits which begin in this manifold remain in it for all time.

The definition used in this work is a slight modification of Rosenberg's, advanced by Kerschen et al.[21] The requirement for vibration in unison is relaxed so that an NNM is a *not-necessarily synchronous periodic motion* of the conservative system. Removing the requirement for synchronous motion admits the possibility of internal resonances – periodic solutions in which modes interact when their frequencies reach integer ratios – as NNMs, and is also useful when pursuing numerical computation of nonlinear modes.

For use with generally applicable algorithms for the numerical continuation of periodic solutions, the nonlinear equations of motion (6) are recast into homogeneous state-space form,

$$\dot{\mathbf{z}} = \mathbf{g}(\mathbf{z}) \tag{16}$$

where the state vector is $\mathbf{z} = [\mathbf{q}^T \ \dot{\mathbf{q}}^T]^T$ and the state function is

$$\mathbf{g}(\mathbf{z}) = \left\{ \begin{array}{c} \dot{\mathbf{q}} \\ -(\bar{\mathbf{M}}^j)^{-1}(\bar{\mathbf{K}}^j\mathbf{q}^j + \boldsymbol{\theta}^j(\mathbf{q}^j)) \end{array} \right\}$$

To emphasize the dependence of the solution on the initial conditions $\mathbf{z}_0$, solutions at a time t are written as $\mathbf{z}(t, \mathbf{z}_0)$. Then, a two-point boundary problem is solved using a periodicity condition,

$$\mathbf{H}(\mathbf{z}_0, T) = \mathbf{z}(T, \mathbf{z}_0) - \mathbf{z}_0 \tag{17}$$

$\mathbf{H}$ is referred to as a *shooting function* and, when driven to zero for a minimal period T, the resulting state vector $\mathbf{z}_0$ corresponds to the initial condition of an NNM of the system. In this work, numerical computation of NNMs was performed using the *NNMcont* MATLAB package, available from the University of Liège website[2] and described by Peeters et al.[22]

Once an NNM is computed from a particular model, its dynamics are compared to the full-order model using a "periodicity" metric. Given any point along the frequency-energy curve, the initial conditions $\mathbf{z}_0$ and period T can be supplied to an FEM and integrated directly. The resulting output, designated $\mathbf{z}_{FE}$, can then be used to obtain a "periodicity error" condition ϵ, defined as

$$\epsilon = \frac{||\mathbf{z}_0 - \mathbf{z}_{FE}||}{||\mathbf{z}_0||} \tag{18}$$

with values on the order of one percent generally taken as acceptable.

4 CASE STUDY

The example structure used here, shown in Figure 1(b), was conceived to meet several requirements while maintaining a minimum level of complexity:

[2]URL: `http://www.ltas-vis.ulg.ac.be/cmsms/index.php?page=nnm`

- Contain at least three components, to expose any effects related to multiple boundary interfaces.
- Use a configuration similar to the panel/stiffener construction used on many aircraft.
- Contain a sufficient number of interface DOF suitable for reduction using CC modes.
- Exhibit strong nonlinear effects in only the "beam" portion of the model.
- Specify no boundary conditions on the "beam" portion in its unassembled state.

This last item turns out to be the most critical, since the geometric nonlinearity of thin beams and panels is intimately related to the boundary conditions of those structures. Further, the ICE method of NLROM generation is not directly applicable to free-free structures. These difficulties are discussed in Section 4.3. First, an overview of the model and its linear representation is presented.

4.1 Structural Model and Linear Substructuring

Two separate assemblies are investigated below. While both have the same general form and use identical structural properties for the beam component, the stiffener thicknesses are modified in each case to obtain slightly different linear dynamic behavior and markedly different nonlinear behavior. The two assemblies are referred to as "soft" and "stiff" in accordance with the different stiffener thicknesses. Structural, material, and mesh properties of the FEM are summarized in Tables 1 and 2.

Part	Young's Modulus [MPa]	Density [$\mathrm{kg/m^3}$]	Thickness [mm]
Panel	71000	2700	1.5
Stiffener [Soft]			
Stiffener [Stiff]			4.0

Table 1: *Material and structural properties of the truncated beam/stiffener assembly components.*

Part	Nodes	S4R Elements	DOF
Panel	182	150	1092
Stiffener [Soft]	105	84	630
Stiffener [Stiff]			
Assembly	392	318	2352

Table 2: *Mesh properties of the truncated beam/stiffener assembly components.*

Five fixed interface modes were retained for the beam and each stiffener; these are shown, along with their corresponding frequencies, in Appendix A. Even though the stiffener modes are at very high frequencies and begin to push the spatial limitations of the coarse mesh, including five FI modes in each stiffener is necessary to obtain more than a handful of modes for the full assembly. Five CC modes were retained for each model and are shown in Table 3. CC mode 1 of each structure is similar to a pinned bending mode – note that the frequency of "soft" CC mode 1 is roughly one quarter the frequency of the "stiff" counterpart. CC mode 4 in each structure is a vertical displacement of the panel on its supports, with the soft structure also showing a rotational displacement of the panel in CC mode 5. By inspection, the most critical modes for panel nonlinearity are CC mode 1 on both structures, mode 2 on the soft structure, and mode 3 on the stiff structure.

Modes of the assembled system are shown in Table 4. Modal assurance criterion (MAC) and frequency error checks are provided in Appendix A and demonstrate that the first five modes of the assembly are comparable to their counterparts from the full-order model. Frequency errors remain below 0.1% for the first five modes of each structure, after which the substructured models immediately lose all accuracy. This results in a frequency range of validity up to 300 Hz, which is sufficient for the nonlinear model desired. The Craig-Bampton substructuring method reduces each model from 2,352 to 99 total degrees of freedom, 84

Table 3: *Characteristic constraint modes of the "soft" (top) and "stiff" (bottom) assembled models.*

Soft Component (1.5 mm Thickness)				
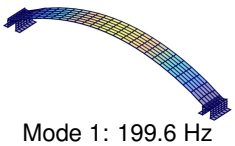 Mode 1: 199.6 Hz	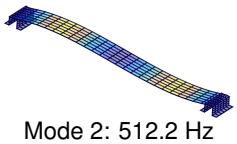 Mode 2: 512.2 Hz	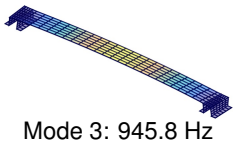 Mode 3: 945.8 Hz	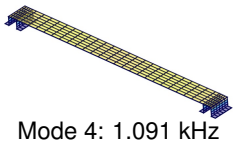 Mode 4: 1.091 kHz	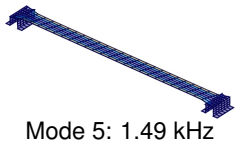 Mode 5: 1.49 kHz
Stiff Component (4mm Thickness)				
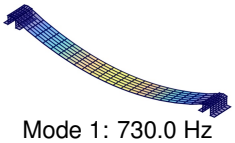 Mode 1: 730.0 Hz	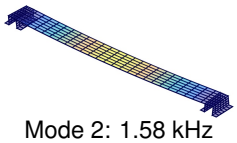 Mode 2: 1.58 kHz	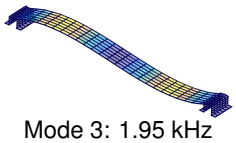 Mode 3: 1.95 kHz	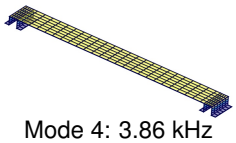 Mode 4: 3.86 kHz	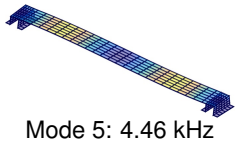 Mode 5: 4.46 kHz

of which are boundary DOF. Attempting to specify a beam NLROM with 89 basis vectors (5 FI modes and 84 constraint modes) would require an untenable 776,384 load cases. By introducing the secondary CC mode reduction, the 84 boundary DOF can be represented using only 5 CC modes, for a total of 20 DOF in the assembly. This means that only 10 basis vectors are required for the panel NLROM, resulting in a much more manageable 1,160 load cases for NLROM specification. It turns out that not all of the FI and CC modes need be included in the model to obtain an accurate first NNM, leading to further reductions in the load case requirements.

Table 4: *Vibration modes of the assembled model, computed with the fixed-interface and characteristic constraint modes shown in Tables 5, 6, and 3*

Soft Component (1.5 mm Thickness)				
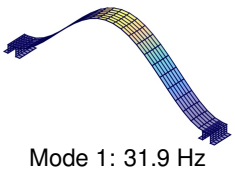 Mode 1: 31.9 Hz	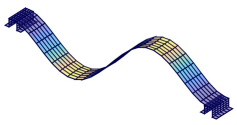 Mode 2: 88.5 Hz	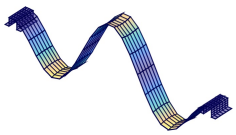 Mode 3: 176.0 Hz	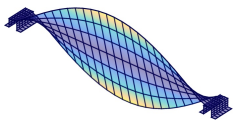 Mode 4: 197.2 Hz	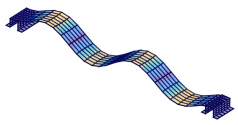 Mode 5: 296.0 Hz
Stiff Component (4mm Thickness)				
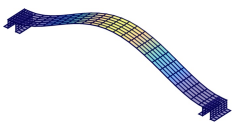 Mode 1: 32.2 Hz	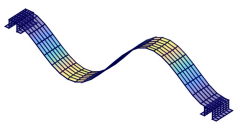 Mode 2: 89.6 Hz	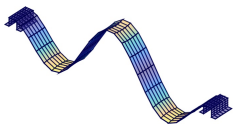 Mode 3: 178.0 Hz	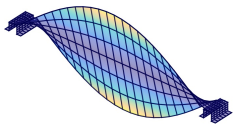 Mode 4: 198.6 Hz	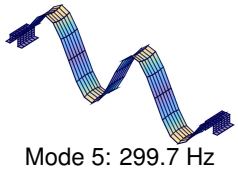 Mode 5: 299.7 Hz

4.2 Reference Nonlinear Model

Before constructing substructured reduced-order models of the assembly, monolithic NLROMs were formed to serve as truth models of the system's nonlinear dynamics. Reduced order models using mode 1 only, modes 1-3, and modes 1-5 were constructed and used to compute the first nonlinear normal mode of each assembly; the resulting NNM backbones for all three NLROMs lie nearly atop one another, as shown in Appendix A, Figures 9 and 10. For reference, an NNM corresponding to a fully-constrained NLROM of the panel only is plotted in Figure 2 along with each assembly's five-mode NLROM, demonstrating that the clamped boundary conditions significantly affect nonlinear behavior of the structure. The stiff model and fully clamped

model have nearly identical linear natural frequencies, indicating that the stiff assembly approximates a “built-in” set of boundary conditions. The soft assembly has a somewhat lower linear natural frequency and displays significantly less nonlinear stiffening – the frequency shift effects do not appear until higher energy levels, and the frequency increases more slowly than the other two models. These three NNM curves are used during inspection of the substructured NLROM results below to better understand the behavior of each assembled model.

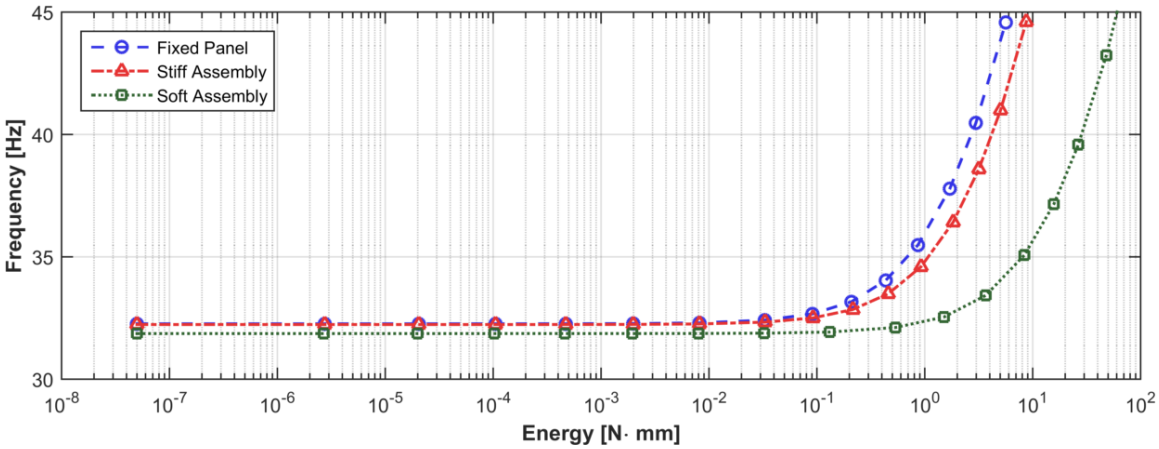

Figure 2: *Truth NNMs of the soft and stiff assemblies along with a fully-fixed FEA model of the panel only.*

4.3 Nonlinear Substructuring

Nonlinear substructuring is conducted on the assumption that only the panel component need be treated as nonlinear, reducing the number of required load cases to specify each NLROM; this assumption is justified based on the extreme natural frequencies of the stiffeners relative to the panel and assembly modes. Only a subset of the lowest FI and CC modes are used to specify the NLROMs, further reducing the number of load cases required for the model.

The key difficulty associated with this model lies in the panel’s lack of boundary conditions in its unassembled state. Immediately this raises an issue with the nonlinear static FEA solutions that must be obtained, since baseline static solvers cannot handle free-free structures. “Inertia relief” (IR) procedures, which allow a static solution by applying forces to eliminate rigid body motion of the structure[23], can overcome this limitation. Unfortunately, the use of IR with the ICE method is not yet well understood. Further, there is a more critical problem to be overcome: physically, nonlinearity of the panel will be dominated by its interaction with the supports, a fact that would not be addressed by using an IR solution procedure. The panel’s FI modes correspond to an unphysical infinite stiffness at the boundaries, while the CC modes are associated with the stiffness of the assembly, statically reduced to the set of boundary nodes. A single, consistent set of boundary conditions must be selected for use in the nonlinear, static FEA routine. Using fully-fixed boundary conditions on FI mode load cases and statically reduced boundary conditions on CC modes is not straightforward, since the modal displacements are inherently coupled and their stiffness coefficients must be estimated in concert with each other.

4.4 Fixed Interface/Characteristic Constraint Mode Basis

With these considerations in mind, it is clear that some combination of alternate procedures must be devised to properly handle the panel in this example. Using the natural basis of FI/CC modes, three possible solutions, listed below, were examined. Once NLROMs were computed using each method, NNMs emanating from the first linear normal mode of each assembly were obtained and compared with the reference modes of Figure 2 to assess the accuracy of the nonlinear models.

- To illustrate the issues caused by inaccurate boundary conditions, an NLROM was constructed using only the fixed-interface modes with fully constrained boundary conditions. The first three panel FI modes were used to construct each NLROM; NNMs resulting from this technique are shown in Figure 3.

- NLROMs were constructed using both FI and CC modes with an approximation of the linear assembly stiffness applied to the boundaries of the panel. This approximation was achieved by statically reducing the assembly stiffness to each boundary DOF on the panel and applying the resulting stiffness values as a set of grounded springs at each degree of freedom. Along with the first three panel FI modes, the first assembly CC mode was included for a pair of NLROMs. The resulting NNMs are shown in Figure 4.
- Finally, loads were applied to the panel within a full FEM of the assembly. This is referred to as an *in situ* technique and is described in further detail below. The resulting NNMs are shown in Figure 5. Again, these NLROMs used a combination of the first three panel FI modes and the first CC mode as a basis set.

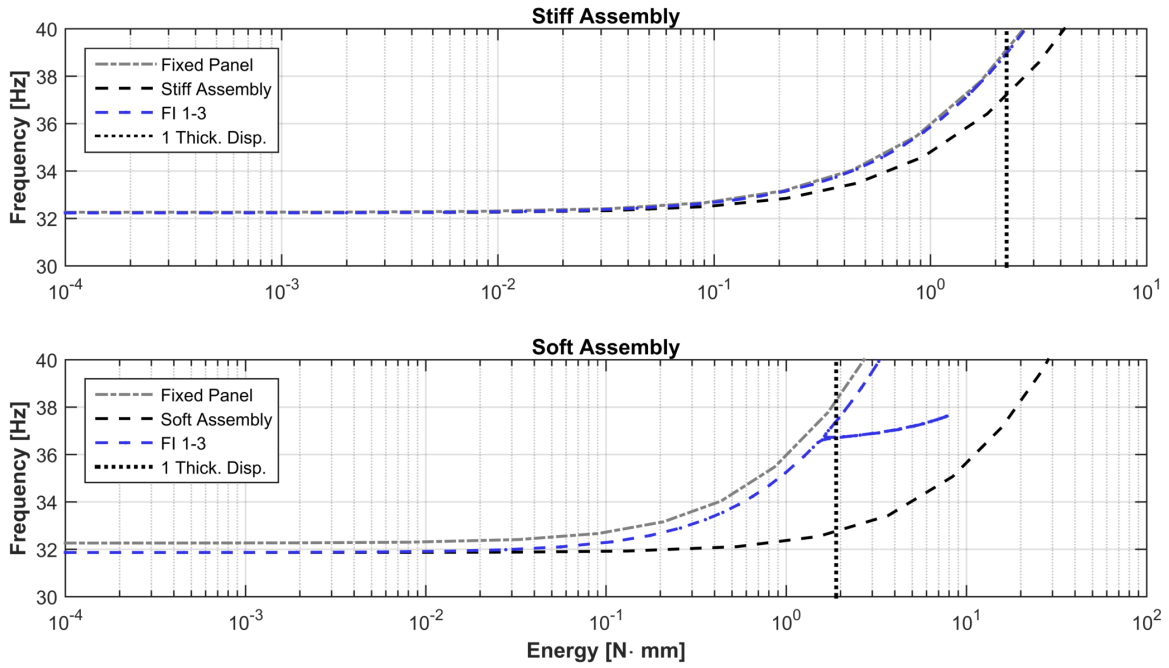

Figure 3: *NNMs computed from substructured NLROMs using only fixed interface modes as a basis for the nonlinear forces and fully-fixed boundary conditions for the ICE load cases.*

Fully Fixed Boundary Conditions

Nonlinear normal modes from the fully fixed case (Figure 3) show NNM backbones tracking closely with the panel-only backbones, indicating that the nonlinear stiffnesses are not determined appropriately when the panel boundaries are fully fixed. Since the linear substructuring is still accurate, the NNM backbone of the soft assembly maintains the correct linear natural frequency at low amplitudes, but ends up tracking the fixed panel's frequency behavior at higher energies. These results are exactly what should be expected from the ICE method, since in neither case is the panel's nonlinear stiffness affected by the underlying stiffness of its boundaries – the FI modes of the panel are identical in both assemblies. Including characteristic CC in the force basis would at least provide some measure of differentiation between the two models; as discussed earlier, however, the CC modes cannot be included if the boundary nodes are fixed, and it is not possible to apply load combinations with FI and CC force vectors if disparate boundary conditions are used on the two subsets of modes. The fixed set of boundary conditions cannot be used to compute component NLROMs for this model.

Linear, Statically Reduced Boundary Conditions

For this case (Figure 4), NNMs associated with the FI-only models show slight softening relative to the fully fixed panel but are still quite far from the desired truth backbones. Additionally, the NNMs computed from the combined FI/CC basis set do not converge

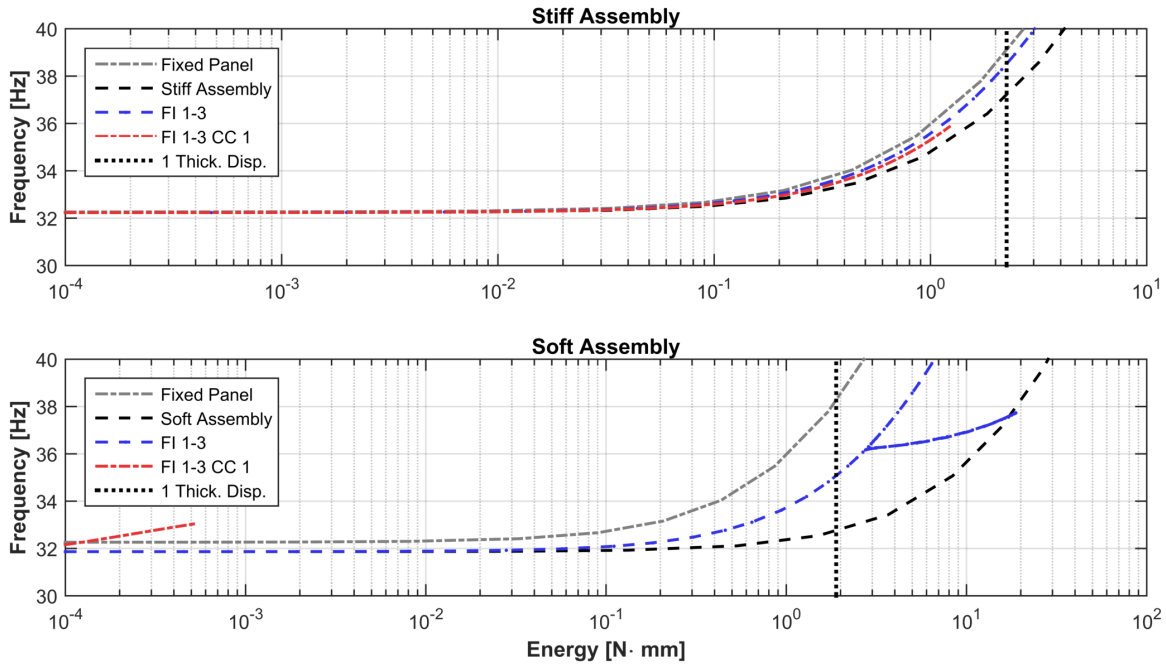

Figure 4: *NNMs computed from substructured NLROMs using FI and CC modes as a basis for the nonlinear forces, with grounded springs applied at the boundaries according to linear, static reduction. In both cases, including CC mode 1 led to a poor nonlinear fit and spurious/non-convergent NNM backbones.*

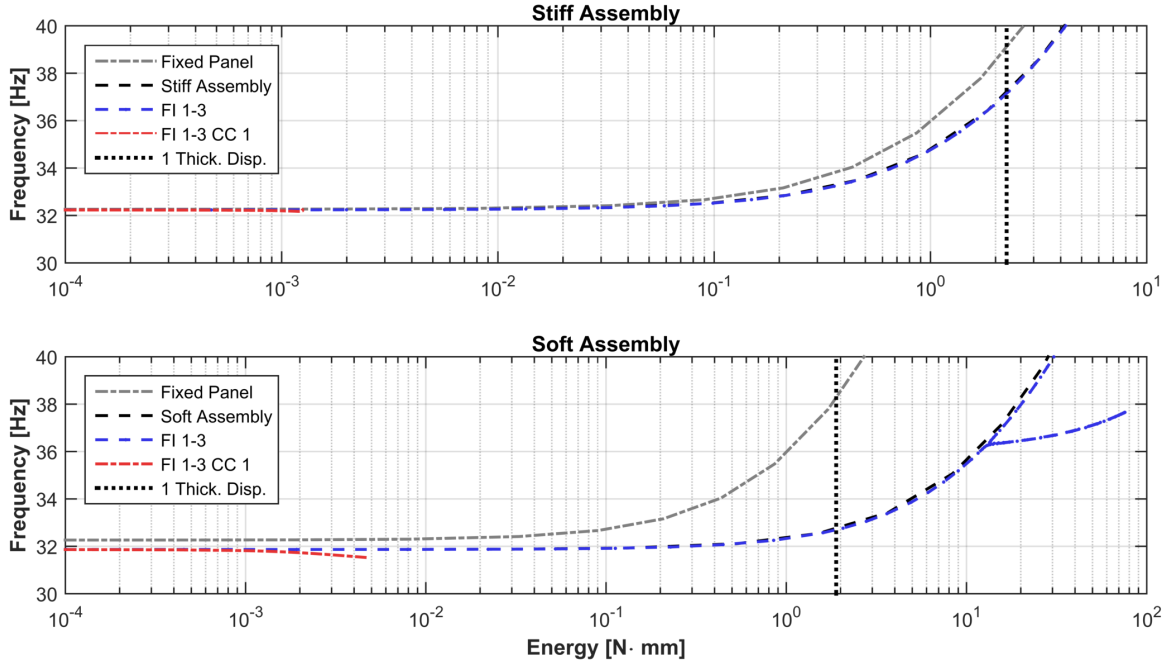

Figure 5: *NNMs computed from substructured NLROMs using FI and CC modes as a basis for the nonlinear forces and the in situ finite element technique to provide accurate boundary stiffness. In both cases, including CC mode 1 led to a poor nonlinear fit and spurious/non-convergent NNM backbone.*

well, with both models failing well before reaching a displacement level of one thickness. Addressing the first issue, the linear approximation to the boundary conditions is clearly insufficiently accurate to produce valid NLROMs using implicit condensation. This is surprising, given that the stiffeners do not undergo large deformations compared to the deformations of the panel, but there is little to be done. Note that the linear approximation includes a static reduction to each individual degree of freedom at the boundary; it remains an open question whether retaining coupling between boundary DOF will lead to an accurate NLROM. This procedure was not attempted due to the difficulty involved in specifying arbitrary stiffness matrices at the boundaries of the FEM. It may also be the case that the boundary stiffness experienced by each node, rather than stiffness coupling between nodes, dominates membrane stretching in the panel. In this case it is the linear boundary approximation itself, rather than the static reduction, that is at fault for the poor models.

In Situ Boundary Conditions

The results above show that a linear approximation to the component boundary conditions is not sufficiently accurate for use with the implicit condensation method. Rather than attempting to formulate more esoteric representations for the boundary stiffness, it is convenient to simply refer to the most accurate possible representation: A full-order FEM of the assembly, which provides a limiting case for the utility of nonlinear substructuring given the most accurate possible component boundaries. The procedure is straightforward: ICE load cases are applied to the subset of DOF corresponding to the component of interest in the FEM, while the remaining DOF are left unloaded. The resulting displacements of that DOF subset are extracted and used in the NLROM construction procedure as per usual, and coefficients of the NLROM are specified in the usual manner. Since it takes place within the full-order model of the assembly, this approach is referred to as the *in situ* substructuring method. The procedure may initially seem indistinguishable from the construction of a monolithic NLROM of the assembly; it is critical to realize that the loads in this instance are being applied only to single components, as opposed to the monolithic approach which uses modes of the entire assembly. Practically speaking, this still dramatically reduces the number of load cases required to specify an NLROM, as discussed in Section 5.

Sets of modes identical to those from Figure 4 were used with the *in situ* procedure and backbones of the first NNM were again generated, with the resulting curves shown in Figure 5. As one would hope, the NNM backbones of the substructured models finally lie close to those of their respective assemblies. The stiff structure shows nearly perfect agreement, although a slight discrepancy and unexpected internal resonance are visible in the NNM backbone of the soft structure. Again, however, models including the first CC mode do not converge to appreciable energy levels.

4.5 QR-Transformed Basis Vectors

The non-convergence of NLROMs including CC modes is a result of the similarity between the structure's first characteristic constraint mode and the beam's first fixed interface mode. The former, with some rotation allowed at the beam interface, resembles a pinned beam mode; the latter is a fully clamped beam mode. Forces applied to the full-order FEM in these mode shapes result in displacements which are difficult to distinguish from each other. As a result, the data matrix used to specify NLROM coefficients is poorly conditioned, and an inaccurate NLROM results.

The QR-transformed basis alleviates this issue by providing an orthogonal set of vectors to use for load case specification. While the FI modes are largely unaffected by the QR decomposition, each CC mode is altered by removing any components that are parallel to any of the fixed interface modes. As a result, the FEM displacements can be reliably distinguished from each other, and deformations at the component interface can be included in the basis.

The NLROMs computed from the QR basis not only converge to suitable energy levels but are more accurate than their counterparts computed with the FI modes only. The resulting backbones of NNM 1 from the QR basis NLROMs are shown in Figure 6. The models shown here use QR modes 1, 2, 3, and 6; these correspond to FI modes 1, 2, and 3, along with the remnant of CC mode 1, which was orthogonal to FI mode 1. The backbone of the stiff structure was already indistinguishable from that of its corresponding assembly NLROM, but the soft assembly backbone has now shifted directly onto the truth curve. Though the difference is slight, the shift is still significant: in a more sophisticated model, omission of constraint deformations could alter the nonlinear dynamics to a much greater extent. For this assembly, only the alternate QR basis was suitable for constructing an NLROM using the implicit condensation procedure.

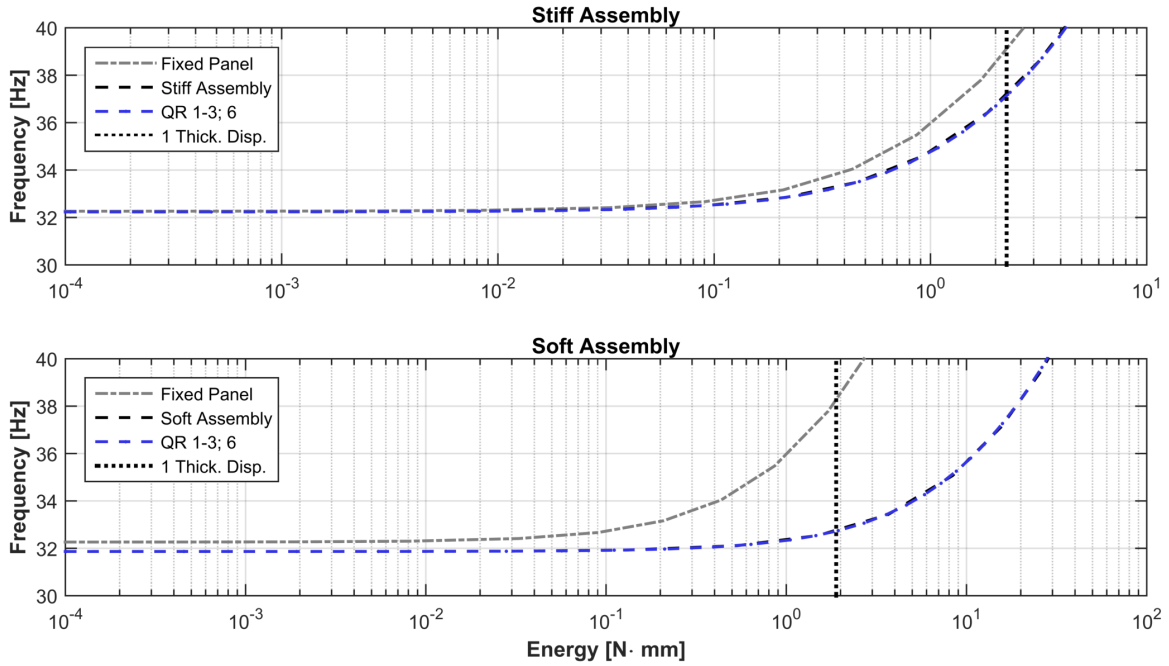

Figure 6: *NNMs computed from substructured NLROMs using vectors from a QR factorization of the FI and CC modeset. Including QR mode 6, corresponding to the component of CC mode 1 which was orthogonal to the FI modes, led to a more accurate NNM for the soft system.*

5 DISCUSSION AND FUTURE PROSPECTS

The panel/stiffener model examined here demonstrated two main challenges that are not encountered in assemblies with fixed-boundary nonlinear components. First, since the key panel component was not constrained in the unassembled state, loads could not be arbitrarily applied to the panel without somehow modifying the boundary conditions. Attempts to model the structure's boundary conditions using linear, statically reduced stiffnesses – grounding springs at each DOF – yielded inaccurate nonlinear models. An important future step is to investigate a fully coupled boundary stiffness at the interface, rather than the single DOF static reduction procedure that was used here. Moving beyond the linear, statically reduced approximation, an *in situ* technique which simply used a full-order FEM of the assembly to describe the component boundary's static behavior during the implicit condensation procedure proved successful.

A second difficulty arose in attempting to include both fixed interface and characteristic constraint modes in the NLROM force basis. The deformations spanned by the first three FI modes and first CC mode were required for an accurate NLROM; however, all models using these four basis vectors led to poor curve fits, due to the similarities between FI and CC mode 1. It is critical to note that, even though the FI and CC modes are nearly orthogonal to each other through the component stiffness matrix, the resulting deformations from a nonlinear static solution are not necessarily well differentiated. As a result, mixing the FI and CC modes led to higher displacement residuals and poor nonlinear coefficient fits.

The alternate basis examined in Section 4.5 was the key to circumventing this issue. Performing a QR factorization of the FI/CC modeset of interest allowed nonlinear force basis resulting in a good coefficient fit to be obtained. Since it allowed inclusion of displacements associated with boundary motion, this basis provided a more accurate NLROM for the assembly on soft supports (the stiff-support version was not noticeably affected). It may be the case that, for panels mounted on stiffeners, force vectors obtained from low-frequency FI and CC modes yield similar displacements. If so, use of an alternate basis such as that obtained from a QR factorization will be critical to obtaining accurate NLROMs of these assemblies.

A remaining question to be addressed is whether a more modular procedure can be devised to take the place of the *in situ* construction process. Component modularity is a key benefit of linear substructuring techniques, allowing manufacturers to share models without exposing proprietary technical parameters. The heavily coupled nature of nonlinear structures, however,

makes it unlikely that full component modularity can be achieved with nonlinear CMS. A more pressing reason for the desire for modularity is based not simply on convenience, but on accuracy of the resulting NLROMs. The case study in this paper contained only a single component exhibiting nonlinearity. When multiple nonlinear components are present in close proximity to each other, loads applied to one component will induce displacements in neighboring parts; it is possible and indeed likely that these displacements will contaminate the nonlinear coefficients obtained for the component of interest. For this reason, the *in situ* procedure with implicit condensation and expansion used here is not yet fully mature or generally applicable to arbitrary assemblies.

The question of efficiency also bears discussion, although it is of less immediate concern. While resorting to a full-order FEM in order to obtain a component NLROM is by no means desirable, it is not a disqualifying requirement. The key benefit of a substructuring approach in specifying NLROMs is the reduction in load cases required to construct a model. Due to the cubic order of growth of these load cases, complicated, built-up geometries which require tens of modes to model quickly become prohibitive. Figure 7 illustrates this principle.

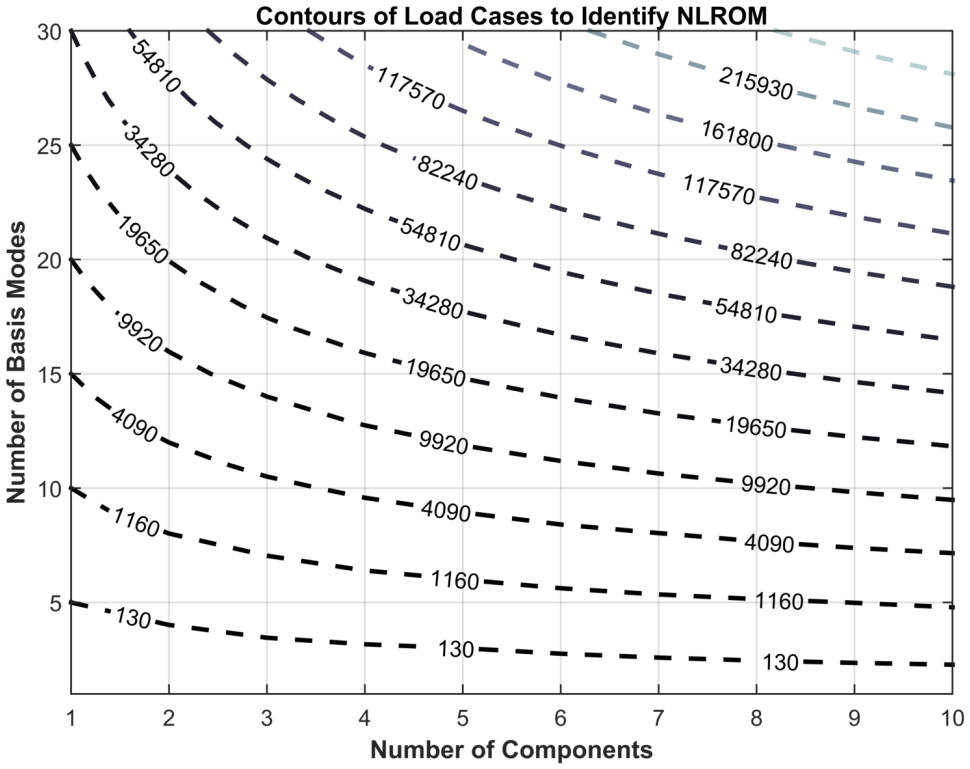

Figure 7: *Contours of required load cases to specify an ICE NLROM as a function of component count and number of basis modes per component. Contours correspond to single-component models at multiples of five basis modes.*

Consider a model which requires 30 modes in the nonlinear basis. A total of 34,280 load cases are required to specify this NLROM. Were the model split into nine nonlinear components, a slightly reduced number of load cases (29,736) would be necessary if each component required 14 modes. Should each component's nonlinear basis be reduced to 10 modes, 10,440 load cases would be needed; at 5 modes, the count drops to 1,160. Even if each of these load cases were run on the full-order FEM, a dramatic savings in construction time would be achieved.

This work has demonstrated the feasibility of applying CMS methods to panel/stiffener assemblies, along with the challenges associated with such a relatively simple extension of prior work. An *in situ* method involving the full-order assembly finite element model was proposed and demonstrated along with the use of alternate basis vectors to specify nonlinear restoring forces. The collection of techniques was sufficient to model an assembly with a single nonlinear component, but further examination along these lines must be conducted before the methods can be generalized to complex models at an industrial scale.

ACKNOWLEDGMENTS

This material is based upon work supported by the National Science Foundation Graduate Research Fellowship under Grant No. DGE-1256259. Any opinion, findings, and conclusions or recommendations expressed in this material are those of the authors(s) and do not necessarily reflect the views of the National Science Foundation.

Support was also provided by the Graduate School and the Office of the Vice Chancellor for Research and Graduate Education at the University of Wisconsin – Madison with funding from the Wisconsin Alumni Research Foundation.

The authors also acknowledge Joseph Hollkamp from the Air Force Research Laboratory's Structural Sciences Center, for the insights that he shared during the conduct of this and other work.

References

[1] R. W. Gordon and J. J. Hollkamp, "Reduced-order models for acoustic response prediction," Tech. Rep. AFRL-RBWP-TR-2011-3040, Air Force Research Laboratory, 2011.

[2] N. Teunisse, P. Tiso, L. Demasi, and R. Cavallaro, "Computational reduced order methods for structurally nonlinear joined wings," in *56th AIAA/ASCE/AHS/ASC Structures, Structural Dynamics, and Materials Conference*, (Kissimmee, Florida), January 2015.

[3] J. Wang, C. Tzikang, D. W. Sleight, and A. Tessler, "Simulating nonlinear deformations of solar sail membranes using explicit time integration," in *45th AIAA/ASCE/AHS/ASC Structures, Structural Dynamics, and Materials Conference*, (Palm Springs, California), March 2004.

[4] E. J. Tuegel, A. R. Ingraffea, T. G. Eason, and M. S. Spottswood, "Reengineering aircraft structural life prediction using a digital twin," *International Journal of Aerospace Engineering*, vol. 2011, 2011.

[5] M. Nash, *Nonlinear Structural Dynamics by Finite Element Modal Synthesis*. PhD thesis, Department of Aeronautics, Imperial College, 1977.

[6] D. J. Segalman and C. R. Dohrmann, "Method for calculating the dynamics of rotating flexible structures, part 1: Derivation," *Journal of Vibration and Acoustics, Transactions of the ASME*, vol. 118, pp. 313–317, 1996.

[7] D. J. Segalman and C. R. Dohrmann, "Method for calculating the dynamics of rotating flexible structures, part 2: Example calculations," *Journal of Vibration and Acoustics, Transactions of the ASME*, vol. 118, pp. 318–322, 1996.

[8] M. I. McEwan, J. Wright, J. E. Cooper, and A. Y. T. Leung, "A combined modal/finite element analysis technique for the dynamic response of a non-linear beam to harmonic excitation," *Journal of Sound and Vibration*, vol. 243, pp. 601–624, 2001.

[9] A. A. Muravyov and S. A. Rizzi, "Determination of nonlinear stiffness with application to random vibration of geometrically nonlinear structures," *Computers and Structures*, vol. 81, pp. 1513–1523, 2003.

[10] M. P. Mignolet, A. Przekop, S. A. Rizzi, and S. M. Spottswood, "A review of indirect/non-intrusive reduced order modeling of nonlinear geometric structures," *Journal of Sound and Vibration*, vol. 332, pp. 2437–2460, 2013.

[11] J. J. Hollkamp, R. W. Gordon, and S. M. Spottswood, "Nonlinear modal models for sonic fatigue response prediction: a comparison of methods," *Journal of Sound and Vibration*, vol. 284, pp. 1145–1163, 2005.

[12] M. C. Bampton and R. R. CRAIG, JR, "Coupling of substructures for dynamic analyses.," *AIAA Journal*, vol. 6, no. 7, pp. 1313–1319, 1968.

[13] R. J. Kuether and M. S. Allen, "Substructuring with nonlinear reduced order models and interface reduction with characteristic constraint modes," in *55th AIAA/ASME/ASCE/AHS/ASC Structures, Structural Dynamics, and Materials Conference*, 2014.

[14] R. J. Kuether, *Nonlinear Modal Substructuring of Geometrically Nonlinear Finite Element Models*. PhD thesis, University of Wisconsin - Madison, 2014.

[15] R. J. Kuether, M. S. Allen, and J. J. Hollkamp, "Modal substructuring of geometrically nonlinear finite-element models," *AIAA Journal*, vol. 54, no. 2, pp. 691–702, 2015.

[16] M. P. Castanier, Y.-C. Tan, and C. Pierre, "Characteristic constraint modes for component mode synthesis," *AIAA journal*, vol. 39, no. 6, pp. 1182–1187, 2001.

[17] J. J. Hollkamp and R. W. Gordon, "Reduced-order models for nonlinear response prediction: Implicit condensation and expansion," *Journal of Sound and Vibration*, vol. 318, pp. 1139–1153, 2008.

[18] M. S. Allen, R. J. Kuether, B. Deaner, and M. W. Sracic, "A numerical continuation method to compute nonlinear normal modes using modal reduction," in *53rd AIAA/ASCE/AHS/ASC Structures, Structural Dynamics, and Materials Conference*, (Honolulu, Hawaii), 2012.

[19] R. M. Rosenberg, "Normal modes of nonlinear dual-mode systems," *Journal of Applied Mechanics*, vol. 27, no. 2, pp. 263–268, 1960.

[20] S. Shaw and C. Pierre, "Normal modes for non-linear vibratory systems," *Journal of sound and vibration*, vol. 164, no. 1, pp. 85–124, 1993.

[21] G. Kerschen, M. Peeters, J. Golinval, and A. F. Vakakis, "Nonlinear normal modes, part i: A useful framework for the structural dynamicist," *Mechanical Systems and Signal Processing*, vol. 23, no. 1, pp. 170–194, 2009.

[22] M. Peeters, R. Viguié, G. Sérandour, G. Kerschen, and J.-C. Golinval, "Nonlinear normal modes, part ii: Toward a practical computation using numerical continuation techniques," *Mechanical systems and signal processing*, vol. 23, no. 1, pp. 195–216, 2009.

[23] Dassault Systems Simulia Corp., *Abaqus Theory Manual*, 2012.

6 APPENDIX A

Various details related to the linear models of the substructure components are given below. Retained fixed interface modes of the panel are given in Table 5.

Table 5: *Retained fixed interface modes of the panel.*

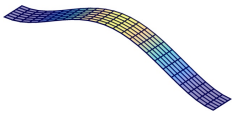 Mode 1: 32.3 Hz	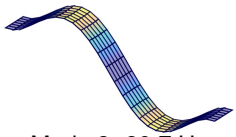 Mode 2: 89.7 Hz	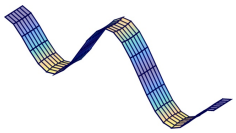 Mode 3: 178.2 Hz	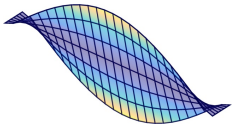 Mode 4: 198.6 Hz	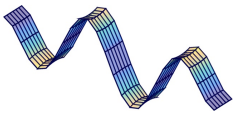 Mode 5: 300.0 Hz

Retained fixed interface modes of the hat stiffeners for soft and stiff assemblies are shown in Table 6.

Table 6: *Retained fixed interface modes of the "soft" (top) and "stiff" (bottom) stiffeners.*

Soft Component (1.5 mm Thickness)				
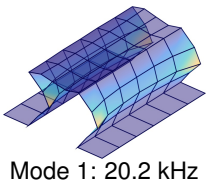 Mode 1: 20.2 kHz	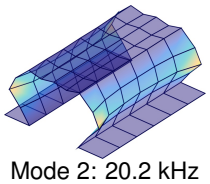 Mode 2: 20.2 kHz	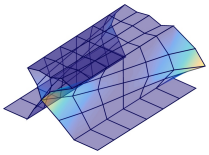 Mode 3: 20.4 kHz	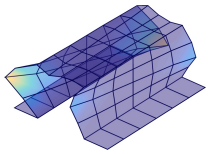 Mode 4: 20.4 kHz	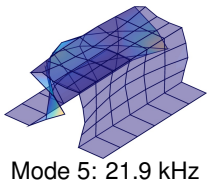 Mode 5: 21.9 kHz
Stiff Component (4mm Thickness)				
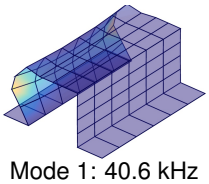 Mode 1: 40.6 kHz	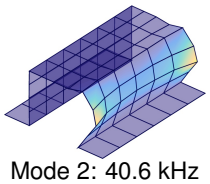 Mode 2: 40.6 kHz	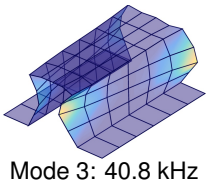 Mode 3: 40.8 kHz	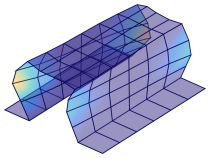 Mode 4: 40.8 kHz	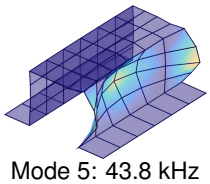 Mode 5: 43.8 kHz

A modal assurance criterion (MAC) check, along with corresponding frequency errors, between the substructured model and its full-order FEA counterpart is given in Figure 8.

Nonlinear normal modes generated using various NLROMs of each assembly, along with the resultant periodicity errors from each model, are shown in Figures 9 and 10 for the stiff and soft assemblies, respectively.

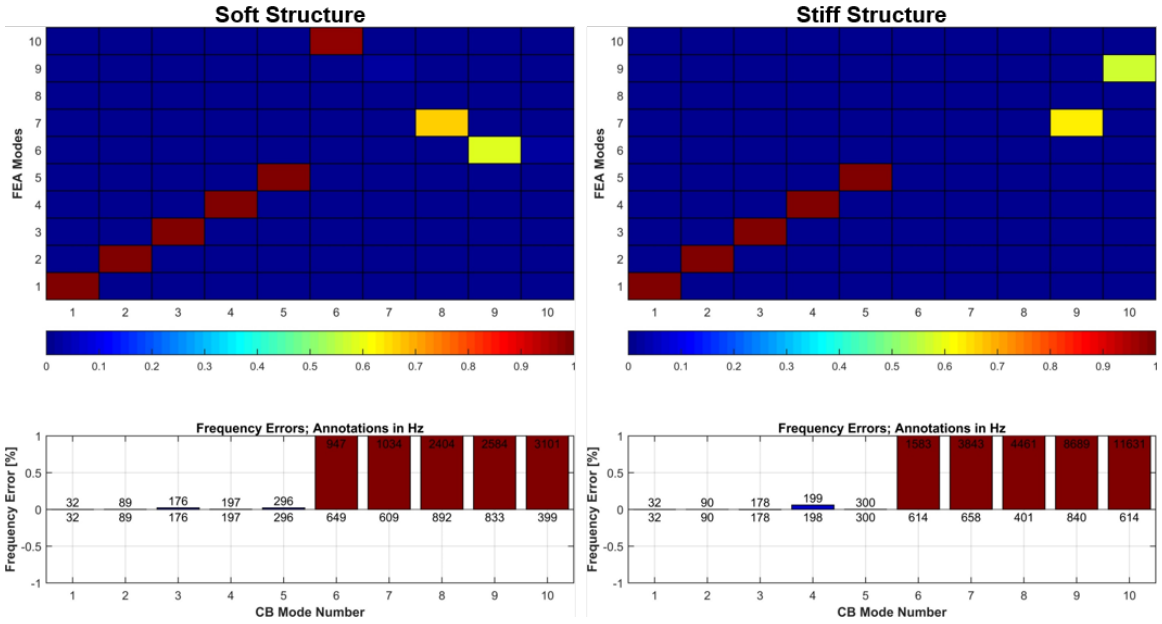

Figure 8: *(Top): Cross-MAC between full-order FEA truth modes and substructure modes. (Bottom): Frequency errors between truth and substructure modes, based on matching MAC value; frequency values along the horizontal axis are full-order values while those adjacent to error bars are the substructured values.*

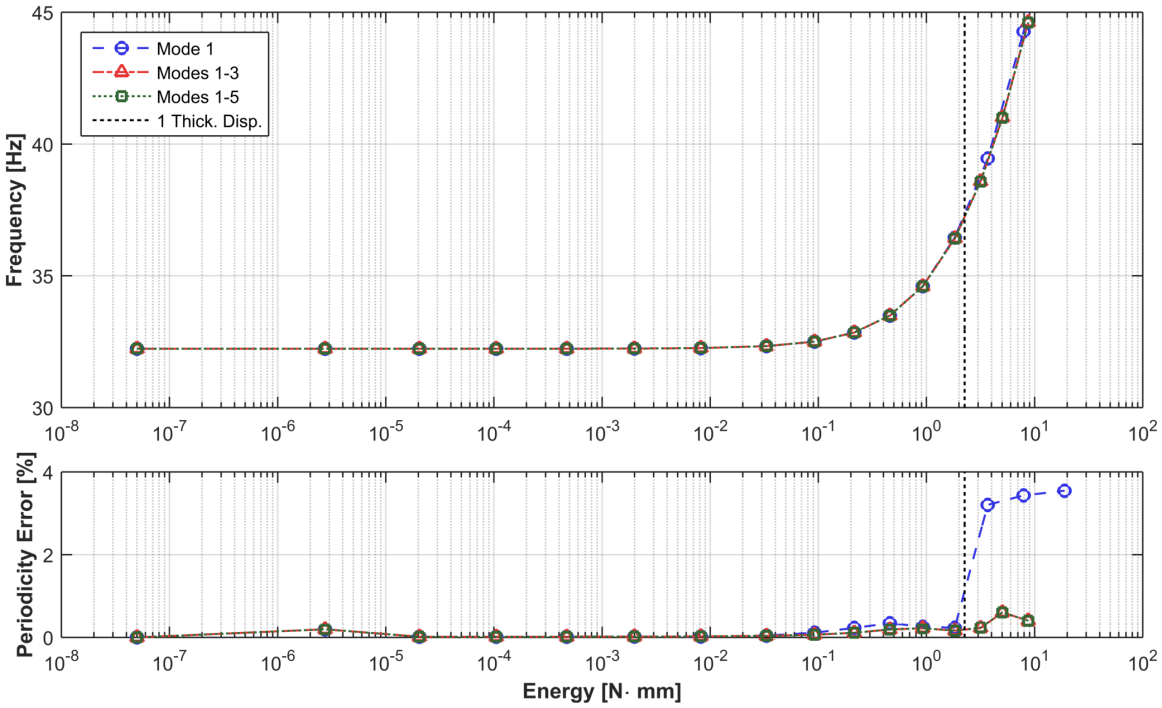

Figure 9: *(Top) NNMs computed using one, three, and five-mode ROMs of a fully assembled FEA model with "stiff" supports. (Bottom) Periodicity errors associated with each computed backbone curve.*

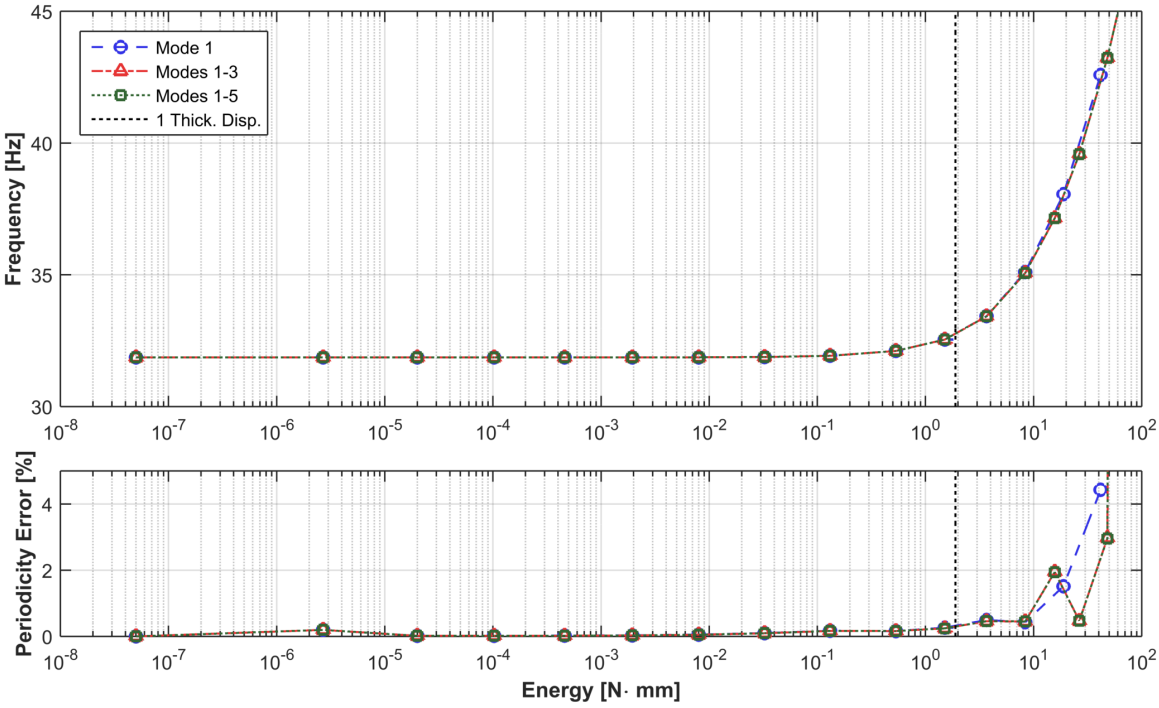

Figure 10: *(Top) NNMs computed using one, three, and five-mode ROMs of a fully assembled FEA model with "soft" supports. (Bottom) Periodicity errors associated with each computed backbone curve.*